Correlation between electron density and temperature in the topside ionosphere

Yoshihiro Kakinami,[1] Shigeto Watanabe,[2] Jann-Yenq Liu,[3,4] and Nanan Balan[3]

Received 2 June 2011; revised 23 October 2011; accepted 24 October 2011; published 31 December 2011.

[1] The correlation between the electron temperature (T_e) and electron density (N_e) at 600 km height at magnetic dip latitudes (MLat) less than about ±40° measured by the Hinotori satellite from February 1981 to June 1982 is presented. The results show the well-known negative correlation between daytime N_e and T_e when N_e is low. However, when the daytime N_e is significantly high (>10^6 cm^{-3}), the correlation turns positive irrespective of latitude, longitude, season, solar flux levels, and magnetic activity levels. The positive correlation is most clear during 1100–1500 local time and around the magnetic dip equator (|MLat| < 10°) where high values of N_e with high T_e are most abundant. T_e also increases with increasing MLat in the same N_e range. Since the cooling through Coulomb collisions increases with the increase of N_e, the results suggest that an additional heat source(s) is involved for the positive correlation between N_e and T_e. The additional heat source seems to be related to the integrated N_e along the magnetic field lines from the ground to 600 km altitude in one hemisphere, which is found to decrease with increasing MLat. Although the mechanism for the positive correlation is not well understood, the results imply that the T_e in the topside ionosphere is controlled more by the integrated N_e than by in situ N_e or F_2 peak N_e.

Citation: Kakinami, Y., S. Watanabe, J.-Y. Liu, and N. Balan (2011), Correlation between electron density and temperature in the topside ionosphere, *J. Geophys. Res.*, *116*, A12331, doi:10.1029/2011JA016905.

1. Introduction

[2] Electron temperature (T_e) in the ionosphere is determined by the heat balance between the heating by photoelectrons, cooling through Coulomb collisions with ions, and heat conduction along the magnetic field lines. Since the photoelectron flux, neutral density [e.g., *Hedin and Mayr*, 1987], and plasma density [e.g., *Lei et al.*, 2005; *Kakinami et al.*, 2009] increase with increasing solar flux, it is not clear whether T_e increases or decreases with an increase in solar flux. Many studies have shown a negative correlation between the electron density (N_e) and T_e during daytime, which is widely accepted [*Evans*, 1971, 1973; *Bilitza*, 1975; *Brace and Theis*, 1978; *Bilitza and Hoegy*, 1990; *Bailey et al.*, 2000; *Zhang and Holt*, 2004; *Zhang et al.*, 2004]. However, a positive or less negative correlation between N_e and T_e under certain conditions has been recently reported. For example, a positive correlation was observed at 850 km in the longitude region between 180°E and 270°E during the December solstice [*Ren et al.*, 2008]. A weak positive correlation was measured using the incoherent scatter radar at Millstone Hill in June [*Zhang and Holt*, 2004]. Further, *Bilitza et al.* [2007] reported N_e and T_e as increasing with increasing solar flux in summer. Theoretical studies have also suggested a positive correlation between N_e and T_e during periods of high solar flux, which is supported with the incoherent scatter data at Arecibo and Millstone Hill [*Lei et al.*, 2007]. According to the explanations of *Lei et al.* [2007], when N_e is sufficiently high, the high cooling that is due to column collisions, the rate of which is proportional to N_e^2 [*Schunk and Nagy*, 1978], leads to a rapid energy transfer from the electrons to the ions and from the ions to the neutrals. These processes result in small temperature differences between electrons, ions, and neutrals. Therefore, electron, ion, and neutral temperatures increase with increasing solar flux because the neutral temperature (T_n) increases as the solar flux increases. That leads to a positive correlation between N_e and T_e because N_e also increases with the increase of solar flux.

[3] Previous studies have concluded that the positive correlation between N_e and T_e accompanies an increase of solar flux [*Lei et al.*, 2007]. However, a recent study indicates that the positive correlation occurs when N_e is significantly high irrespective of solar flux [*Kakinami et al.*, 2011]. The result implies that N_e is an important factor that determines T_e in the topside ionosphere. Further, since an exponential reduction of N_e above the F_2 layer peak leads to a decrease in the cooling by means of Coulomb collisions, heat conduction along the field lines becomes important in

[1]Institute of Seismology and Volcanology, Hokkaido University, Sapporo, Japan.
[2]Department of Cosmoscience, Hokkaido University, Sapporo, Japan.
[3]Institute of Space Science, National Central University, Jhongli, Taiwan.
[4]Also at Center for Space and Remote Sensing Research, National Central University, Jhongli, Taiwan.

0148-0227/11/2011JA016905

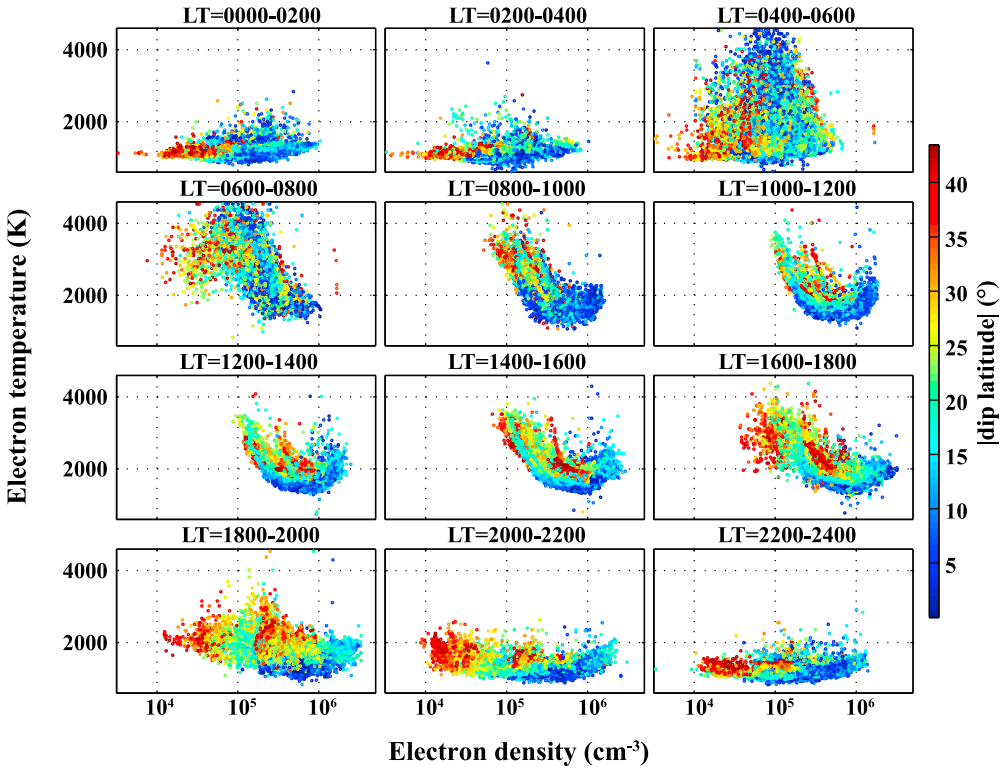

Figure 1. Correlation between T_e and N_e under geomagnetically quiet conditions (K_p < 3) in 2 h LT intervals. Color indicates absolute values of magnetic dip latitude.

the topside ionosphere [*Bilitza et al.*, 2007]. In this paper, we present the correlation between N_e and T_e in the topside ionosphere at 600 km height in ±40° MLat measured by the Hinotori satellite. The correlation between N_e and T_e turns positive when N_e becomes high. The dependence of the positive correlation on different geophysical conditions is studied. The possible reasons for the positive correlation are also discussed.

2. Data and Analytical Results

[4] The Hinotori satellite, launched in February 1981, had a circular orbit of a period of about 90 min, altitude 600 km, and inclination 31°. The orbits covered geographic latitudes within ±32° equally for all longitudes except the southern Pacific and northern Antarctica [*Kakinami et al.*, 2008]. N_e and T_e were independently measured for 16 months until June 1982 using an impedance probe for electron density [*Oya et al.*, 1986] and a resonance rectification probe for electron temperature [*Hirao and Oyama*, 1970; *Oyama et al.*, 1999]. The solar flux index $F_{10.7}$ (in 10^{-22} W/m^2 Hz) during the period of observation was between 143 and 305, with an average of 214.

[5] The correlation between N_e and T_e under geomagnetically quiet conditions (K_p < 3) in the topside ionosphere in 2 h local time (LT) intervals is shown in Figure 1 with a color code for magnetic dip latitudes (MLats). As shown, T_e rapidly increases with the onset of photoelectron heating during sunrise (0400–0600 LT). The rapid T_e increase is called morning overshoot [e.g., *Oyama et al.*, 1996a]. The onset time of the morning overshoot depends on season and latitude [*Kakinami et al.*, 2010]. After sunrise, the relation between N_e and T_e becomes an "inverted U shape" during 0600–0800 LT (Figure 1) with the peak T_e occurring for an N_e of about 10^5 cm^{-3}. The inverted U shape arises from the positive correlation for lower N_e, and a negative correlation for higher N_e is expected during daytime. Also, during this period (0600–0800 LT) N_e lower than 10^5 cm^{-3} are mainly observed outside the magnetic dip equator region (color code in Figure 1).

[6] As local time advances, the relation between N_e and T_e changes to a U shape during 1000–1600 LT (Figure 1). The U-shape relation includes a negative correlation for lower values of N_e and a positive correlation for higher values of N_e. The negative correlation, which is expected during daytime, has been reported by a number of scientists [e.g., *Bilitza*, 1975; *Brace and Theis*, 1978]. The positive correlation, which is observed for high values of N_e, is a new aspect of the present paper. As shown by the color code in Figure 1, the positive correlation is most clear around the magnetic dip equator, where high values of N_e are most abundant. The U-shape relation with positive correlations for high values of N_e is also most pronounced during 1100–1500 LT, as illustrated in Figure 2. After about 1600 LT the U-shape relation gradually disappears (Figure 1). After about 2000 LT, both N_e and T_e follow the usual nighttime decay until sunrise and a positive correlation between N_e and T_e is detected. A similar positive correlation between N_e and T_e was detected using the incoherent scatter radar at Saint Santin [*Zhang et al.*, 2004].

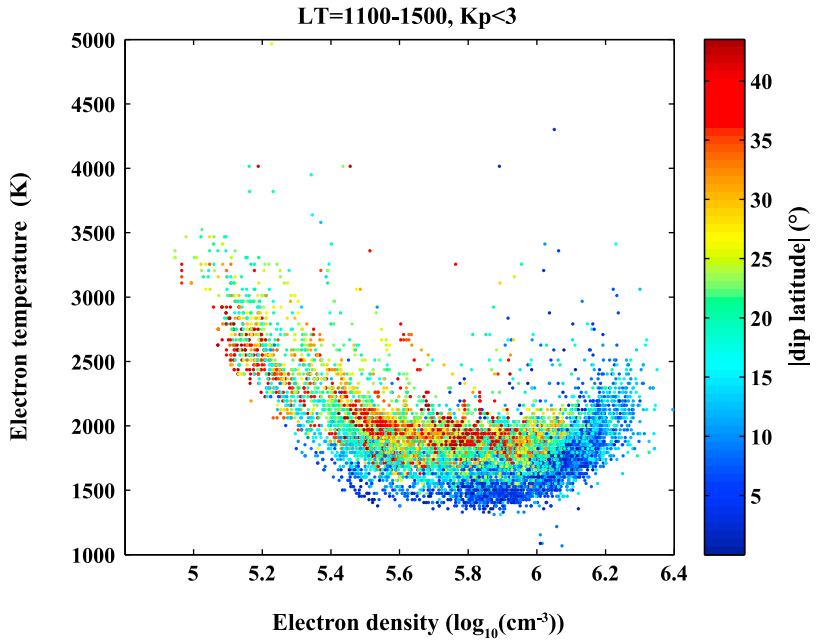

Figure 2. The same as Figure 1, but for LT = 1100–1500.

[7] Next we check the dependence of the positive correlation between N_e and T_e on latitude, longitude, season, solar flux levels, and magnetic activity levels. Figure 3 shows the latitudinal dependence of the U-shape relation between N_e and T_e using the data during 1000–1600 LT under magnetically quiet conditions (K_p < 3). Although the U shapes are detected in all six latitude ranges, the positive correlation between N_e and T_e is clear in the equatorial ionization anomaly (EIA) latitudes within about ±20° MLat [*Namba and Maeda*, 1939; *Appleton*, 1946], where high values of N_e with high T_e are most abundant; the high N_e at 600 km height is due to the strongest photoionization around the

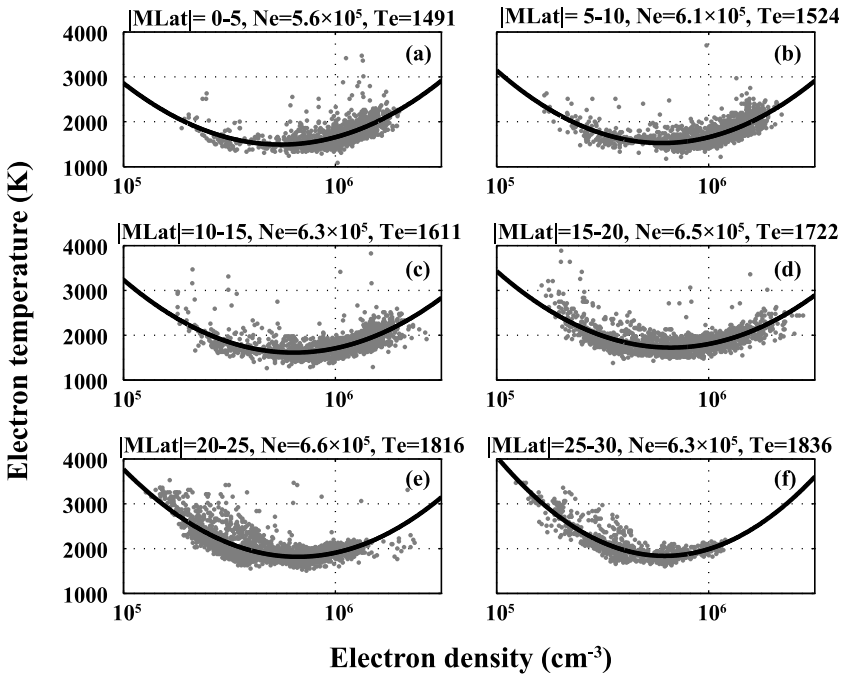

Figure 3. Magnetic dip latitude dependence of the correlation between N_e and T_e during 1000–1600 LT under geomagnetically quiet conditions (K_p < 3). The ranges of absolute magnetic dip latitude are (a) 0°–5°, (b) 5°–10°, (c) 10°–15°, (d) 15°–20°, (e) 20°–25°, and (f) 25°–30°. The curves are fitted with least squares fitting using a quadratic function. Values of N_e and T_e at the top of each graph denote threshold values at which the correlation changes from negative to positive.

Table 1. Magnetic Latitudinal Variations of Threshold Values of N_e and T_e Between Negative and Positive Correlations Shown in Figure 3

	|MLat|					
	0°–5°	5°–10°	10°–15°	15°–20°	20°–25°	25°–30°
N_e (cm^{-3})	5.6×10^5	6.1×10^5	6.3×10^5	6.5×10^5	6.6×10^5	6.3×10^5
T_e (K)	1491	1524	1611	1722	1816	1836

Table 2. Longitudinal Variations of Threshold Values of N_e and T_e Between Negative and Positive Correlations Shown in Figure 4

	Longitude			
	0°–90°	90°–180°	180°–270°	270°–360°
N_e (cm^{-3})	6.2×10^5	5.9×10^5	5.4×10^5	5.4×10^5
T_e (K)	1587	1532	1449	1520

equator and upward $\mathbf{E} \times \mathbf{B}$ drift or forward plasma fountain [*Moffett and Hanson*, 1965; *Balan and Bailey*, 1995]. Threshold values of logarithmic N_e and T_e at which the correlation changes from negative to positive are calculated with least squares fitting using a quadratic function (Table 1). The threshold values of both N_e and T_e increase with increasing MLat.

[8] Figure 4 displays the correlation between N_e and T_e in 90° longitudinal intervals using the data in |MLat| < 10° during 1000–1600 LT under magnetically quiet conditions ($K_p < 3$). Almost the same U-shape relation is observed in all longitudes. In other words, the positive correlation between N_e and T_e seems to be independent of longitude. However, the threshold values of N_e and T_e seem to depend on longitude. The threshold values of both N_e and T_e are lowest in the 180°E–270°E longitudes (Table 2).

[9] The seasonal dependence of the correlation between N_e and T_e in three latitude ranges covering magnetic north and south are shown in Figure 5; the data during 1000–1600 LT under $K_p < 3$ are used. As shown, the positive correlation between N_e and T_e is observed in all seasons around the equator (|MLat| < 10°) where high values of N_e are present. The positive correlation also exists at higher latitudes (|MLat| between 10° and 30°) but mainly in winter and at equinoxes when high values of N_e are abundant. Meanwhile, in the summer months, the positive correlation is not clear when high values of N_e are less. The seasonal dependence also indicates a clear positive correlation between N_e and T_e when N_e is high.

[10] Figure 6 displays the solar flux dependence of the correlation between N_e and T_e. The variations of N_e with T_e are plotted for different $F_{10.7}$ ranges using the data in |MLat| < 10° during 1000–1600 LT under magnetically quiet conditions ($K_p < 3$). The U-shape relation with positive correlations is observed in all $F_{10.7}$ ranges though low values of N_e for high levels of $F_{10.7}$ are less abundant. The threshold values of N_e and T_e for the different solar flux levels are listed in Table 3. The threshold of T_e increases steadily with the increase in solar flux while that of N_e undergoes a fluctuation with the lowest value in the 200–250 flux range, which may be related to the saturation of N_e with $F_{10.7}$ [*Balan et al.*, 1993].

[11] The dependence of the correlation between N_e and T_e on different geomagnetic activity levels is also examined (Figure 7). Similar U-shape relations are observed at all levels of K_p, though the negative correlation between them is hard to detect for K_p greater than 6 because of the smaller number of lower values of N_e. The results imply that the positive correlation between N_e and T_e for high N_e is independent of magnetic activity. The threshold values of N_e and T_e listed in Table 4 are higher for higher ranges of K_p except for the highest range ($K_p > 6$). Because of the small number

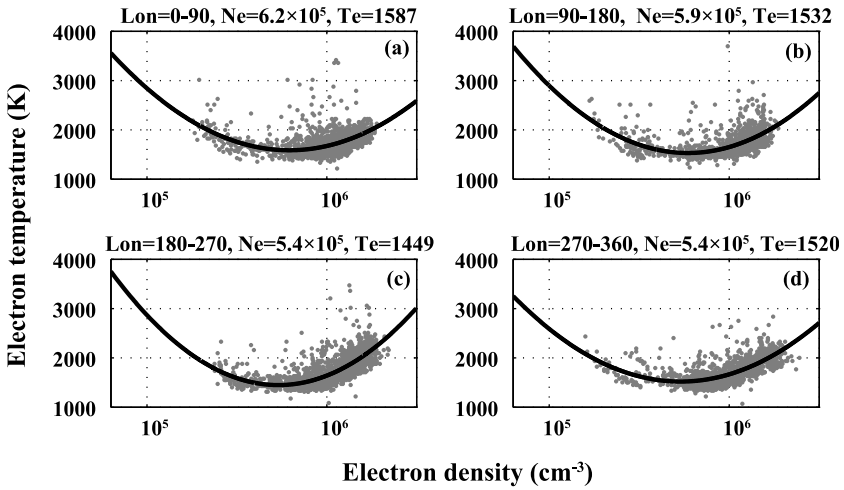

Figure 4. Longitudinal dependence of the correlation between N_e and T_e in |MLat| < 10° during 1000–1600 LT under geomagnetically quiet conditions ($K_p < 3$). Longitudinal ranges are (a) 0°–90°, (b) 90°–180°, (c) 180°–270°, and (d) 270°–360°. The curves are fitted with least squares fitting using a quadratic function. Values of N_e and T_e at the top of each graph denote threshold values at which the correlation changes from negative to positive.

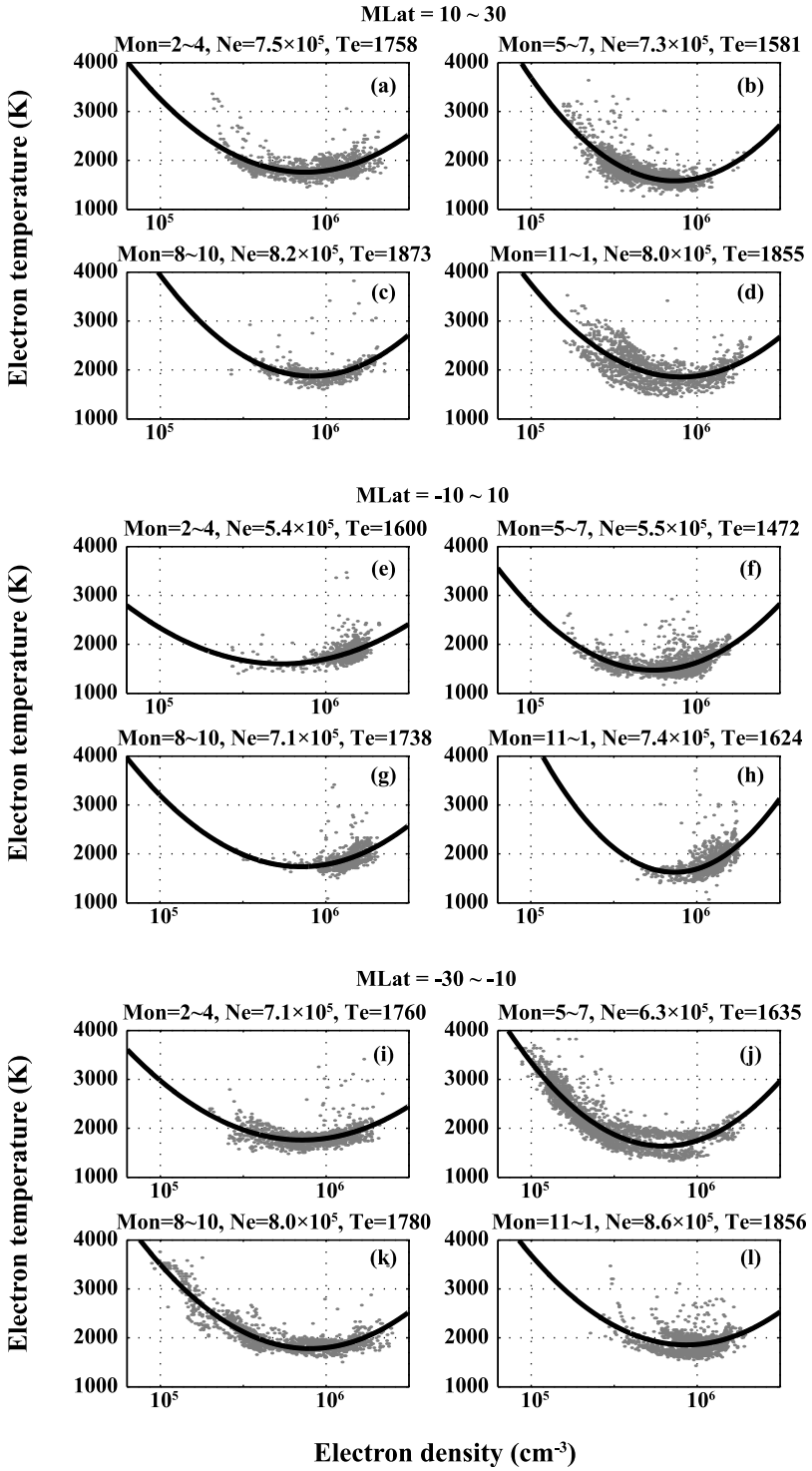

Figure 5. Seasonal dependence of the correlation between N_e and T_e in MLat = (a–d) 10°∼30°, (e, f) −10°∼10°, and (i–l) −30°∼−10°. "Mon" denotes months for which data are accumulated. The curves are fitted with least squares fitting using a quadratic function. Values of N_e and T_e at the top of each graph denote threshold values at which the correlation changes from negative to positive.

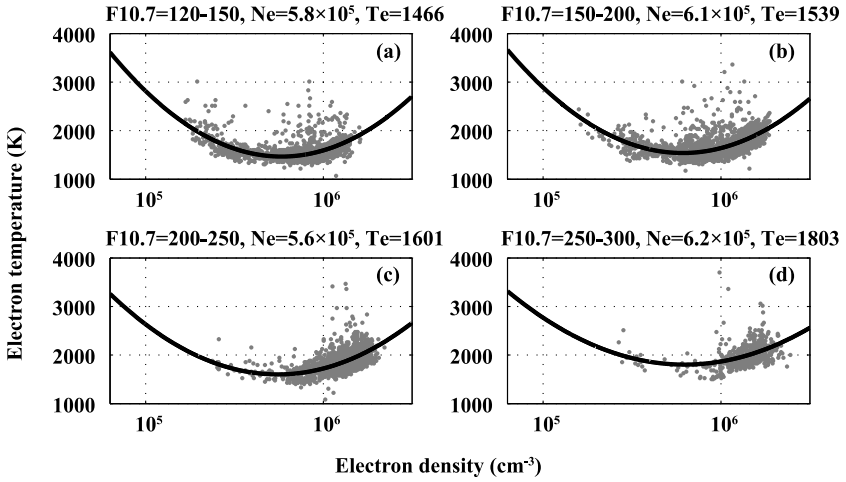

Figure 6. Solar flux dependence of the correlation between N_e and T_e in |MLat| < 10° during 1000–1600 LT under geomagnetically quiet conditions (K_p < 3). $F_{10.7}$ ranges are (a) 120–150, (b) 150–200, (c) 200–250, and (d) 250–300. The curves are fitted with least squares fitting using a quadratic function. Values of N_e and T_e at the top of each graph denote threshold values at which the correlation changes from negative to positive.

of low N_e, it is hard to obtain accurate threshold values for K_p > 6.

3. Discussion

[12] The N_e and T_e data in the topside ionosphere (~600 km height) measured by the Hinotori satellite presented above reveal a positive correlation between them for high values of N_e (>10^6 cm^{-3}) during daytime (1000–1600 LT). The positive correlation is most clear during 1100–1500 LT and around the equator (|MLat| < 10°) where high values of N_e with high T_e are most abundant in all longitudes, all seasons, and all levels of solar activity ($F_{10.7}$ > 120) and magnetic activity. The positive correlation is also present at higher latitudes (|MLat| < 30°) when N_e exceeds the threshold limit. Further, T_e in the same N_e range decreases with increasing MLat. The possible reasons for the positive correlation are discussed below after addressing a similar earlier study.

[13] *Lei et al.*, [2007] reported the positive correlation between N_e and T_e at F_2 peak height using the incoherent scatter radar data at Millstone Hill and Arecibo. They also supported the observations through numerical simulations. According to their interpretation, since the cooling through Coulomb collisions is strong when N_e is sufficiently high, the differences in the temperatures of electrons, ions, and neutrals decrease with the increase of N_e when solar flux is high. Hence the positive correlation between N_e and T_e appears with increasing solar flux because both T_n and N_e increase with increasing solar flux. However, our results show that the positive correlation appears in all solar flux levels, $F_{10.7}$ > 120 (Figure 6). Further, the positive correlation is present in all seasons when N_e is sufficiently high and is centered at equatorial latitudes.

[14] The heat budget of electrons in the ionosphere is governed by photoelectron heating, cooling by means of collisions with ions and neutrals, and heat conduction along magnetic field lines. Since electrons are primarily cooled by collisions with neutrals below about 200 km altitudes [*Bilitza*, 1987], T_e is nearly independent of N_e [*Brace and Theis*, 1978]. Meanwhile, the electrons are cooled through the Coulomb collisions with ions at higher altitudes because plasma density increases with an increase of altitude below the F_2 peak while neutral density decreases. Therefore, T_e is strongly dependent on N_e; it is also negatively correlated with N_e when cooling by Coulomb collisions is dominant. Since N_e exponentially decreases with increasing altitude above the F_2 layer peak, local cooling due to the Coulomb collisions decreases and heat conduction becomes dominant as the altitude increases [*Bilitza et al.*, 2007]. Therefore, cooling around the F_2 peak is also important for T_e in the topside ionosphere. N_e at the F_2 peak shows the EIA structure while integrated N_e along the magnetic field line from the ground to satellite altitude in one hemisphere decreases with an increase of MLat (Figure 8). T_e in the same N_e range increases with increasing MLat during daytime (Figures 1–3). Our results therefore suggest that the integrated N_e becomes important in the topside ionosphere where heat conduction is dominant because T_e does not show an EIA-like structure. These facts imply that T_e in the topside ionosphere does not fully depend on in situ N_e and F_2 peak N_e.

[15] Photoelectron heating rate is known to increase with the increase of ambient plasma density [*Hoegy*, 1984]. Also, the energy dissipation of photoelectrons is proportional to integrated N_e along the magnetic field lines which the photoelectron passes through [*Nagy and Banks*, 1970]. Further, since the heating rate of electrons by photoelectrons is inversely proportional to the square root of the mean energy of photoelectrons because of the inverse proportion

Table 3. Solar Flux $F_{10.7}$ Variations of Threshold Values of N_e and T_e Between Negative and Positive Correlations Shown in Figure 6

	$F_{10.7}$			
	120–150	150–200	200–250	250–300
N_e (cm^{-3})	5.8 × 10^5	6.1 × 10^5	5.6 × 10^5	6.2 × 10^5
T_e (K)	1466	1539	1601	1803

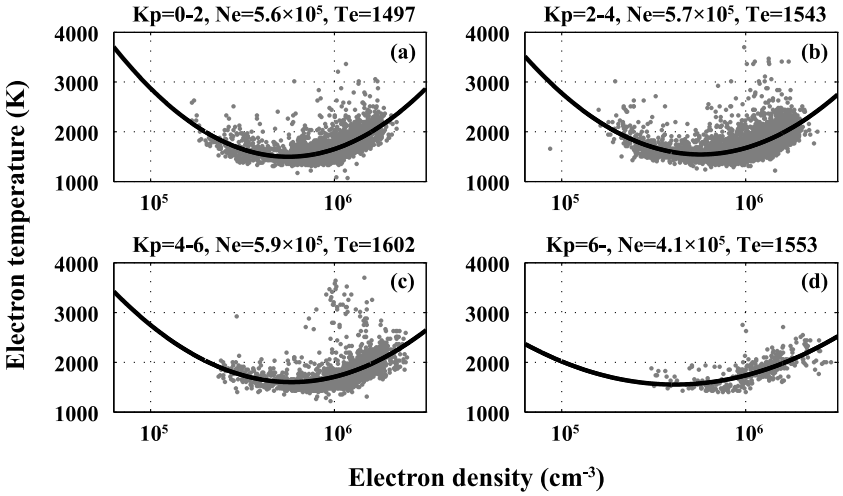

Figure 7. Dependency of correlation between N_e and T_e on geomagnetic disturbances in |MLat| < 10° during 1000–1600 LT. K_p ranges are (a) 0–2, (b) 2–4, (c) 4–6, and (d) greater than 6. The curves are fitted with least squares fitting using a quadratic function. Values of N_e and T_e at the top of each graph denote threshold values at which the correlation changes from negative to positive.

of electron-electron collision cross sections to its energy [*Mantas*, 1975], the heating rate of electrons is possibly high in the region where the integrated N_e is high. These facts therefore indicate that the total heating rate of photoelectrons increase with the increase of integrated N_e.

[16] Because both the cooling and heating rates increase with the integrated N_e, it is difficult to conclude which effect is important to determine T_e in the topside ionosphere. However, our results show that a similar structure of the correlation between N_e and T_e is observed in all magnetic dip latitudes (Figure 3), longitudes (Figure 4), seasons (Figure 5), and solar flux levels (Figure 6) when N_e exceeds the threshold limit. Further, the correlations are similarly observed in all K_p levels (Figure 7). These results suggest that T_e is mainly controlled by the integrated N_e even during magnetic storms. Since the heating rate abruptly increases when the field line length is less than a specific length [*Kakinami et al.*, 2010], the heating rate dominates the cooling rate of electrons. These facts therefore imply that additional heat sources are involved in accompanying the integrated N_e enhancement and possibly explain that a positive correlation appears between N_e and T_e when N_e exceeds the threshold limit.

[17] The threshold values of N_e and T_e increase with increasing solar flux levels and magnetic disturbance. However, the dependence of the threshold values on longitudes shows a minimum value in the 180°–270° longitude. Although variations of the threshold value are not well understood, the integrated N_e and T_n possibly affect them because the integrated N_e possibly controls heating and cooling rates, and T_n becomes a base temperature for ions and electrons through the cooling process.

[18] Another positive correlation is observed during the morning overshoot period when N_e is less than about 8×10^4 cm^{-3}; this is observed mainly out of the EIA region. The heating of the lower ionosphere by the photoelectrons is strongly dependent on the solar zenith angle (SZA) during the morning overshoot of T_e [*Dalgarno and McElroy*, 1965]. Although a rapid decrease in SZA causes a rapid increase of heating rate at low latitudes, the heating at higher latitudes gradually increases because of the gradual increase in SZA as LT advances. Since both N_e and heating by photoelectrons increase as SZA increases, the positive correlation between T_e and N_e during the morning overshoot arises from the LT variation of the heating by photoelectrons.

4. Conclusion

[19] We investigated the correlation between N_e and T_e at 600 km height at magnetic dip latitudes less than about ±40° using the Hinotori satellite data from February 1981 to June 1982. An expected inverse U shape and a new U-shape relationship are seen in the correlation plots of N_e and T_e during early morning (0600–0800 LT) and daytime (1000–1600 LT) hours, respectively. The U-shape relation is observed in all longitudes, latitudes, seasons, solar flux levels, and magnetic disturbance levels, though it is most clear around the magnetic dip equator during 1100–1500 LT. Threshold values of N_e and T_e at which the positive correlation begins increase with MLat, solar flux, and magnetic disturbance, and show the lowest values in the 180°E–270°E longitude range. Further, T_e in the same N_e range increases with increasing MLat. Since the cooling through Coulomb collisions increases with the increase of N_e, an additional heat source(s) is required for the positive correlation between N_e and T_e. The integrated N_e decreases with an increase of MLat while in situ N_e as well as F_2 peak N_e shows the EIA structure. Therefore, these results indicate that T_e in the

Table 4. Magnetic Disturbance K_p Variations of Threshold Values of N_e and T_e Between Negative and Positive Correlations Shown in Figure 7

	K_p			
	0–2	2–4	4–6	>6
N_e (cm^{-3})	5.6×10^5	5.7×10^5	5.9×10^5	4.1×10^5
T_e (K)	1497	1543	1602	1553

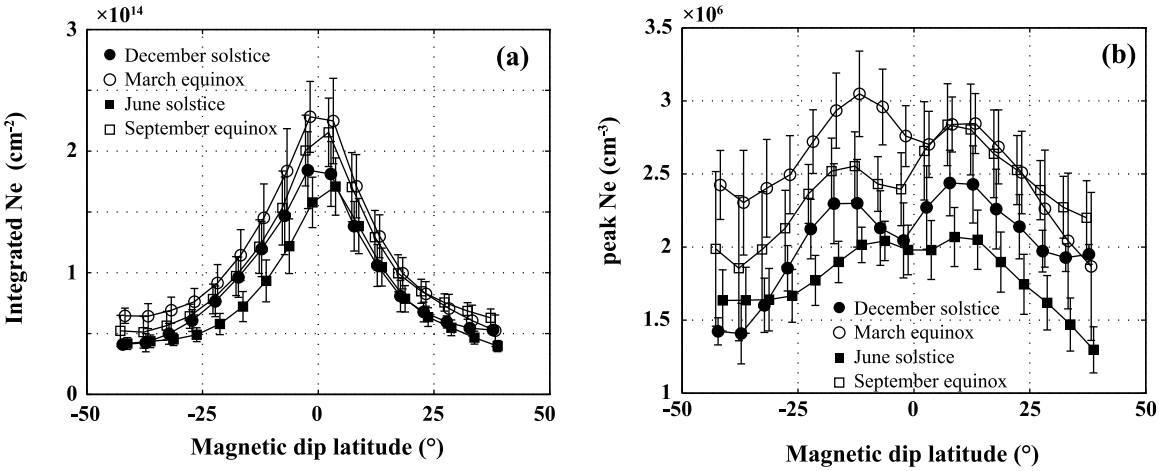

Figure 8. (a) Integrated N_e along a flux tube from the ground to 600 km altitude in one hemisphere with respect to magnetic dip latitude and (b) peak N_e for 1200 LT. Magnetic dip latitudes correspond to the satellite altitude, 600 km. Integrated N_e and peak N_e are calculated using IRI2007 and IGRF for 1981. Data cover every 30° in longitude and 2.5° in latitude for every month. Symbols denote seasons. Error bars display standard deviations.

topside ionosphere is controlled more by the integrated N_e along the magnetic field line from the ground to 600 km height than by in situ N_e or F_2 peak N_e. Although many factors such as the daytime upward **E** × **B** drift, neutral winds in the thermosphere, and waves of tropospheric origin also affect the in situ N_e in the topside ionosphere and F_2 peak N_e [*Fejer*, 1991; *Oyama et al.*, 1996b; *Watanabe and Oyama*, 1996; *Kakinami et al.*, 2011], our results indicate that T_e in the low-latitude topside ionosphere is possibly controlled by photoelectron heating and cooling through Coulomb collisions with ions that are related to the integrated N_e.

[20] **Acknowledgments.** The authors thank two anonymous reviewers for their constructive comments. The authors also would like to express our sincere appreciation to all members of the Hinotori satellite project. This work was partially supported by Earth Observation Research Center, Japan Aerospace Exploration Agency (Y. K. and S. W.) and the National Science Council project NSC 98-2116-M-008-006-MY3 grant of the National Central University (Y. K. and J. Y. L.).

[21] Robert Lysak thanks the reviewers for their assistance in evaluating this paper.

References

Appleton, E. V. (1946), Two anomalies in the ionosphere, *Nature*, *157*, 691, doi:10.1038/157691a0.

Bailey, G. J., Y. Z. Su, and K.-I. Oyama (2000), Yearly variations in the low-latitude topside ionosphere, *Ann. Geophys.*, *18*, 789–798, doi:10.1007/s00585-000-0789-0.

Balan, N., and G. J. Bailey (1995), Equatorial plasma fountain and its effects: Possibility of an additional layer, *J. Geophys. Res.*, *100*, 21,421–21,432, doi:10.1029/95JA01555.

Balan, N., G. J. Bailey, and B. Jayachandran (1993), Ionospheric evidence for a non-linear relationship between the solar EUV and 10.7 cm fluxes during an intense solar cycle, *Planet. Space Sci.*, *41*, 141–145, doi:10.1016/0032-0633(93)90043-2.

Bilitza, D. (1975), Models for the relationship between electron density and temperature in the upper ionosphere, *J. Atmos. Terr. Phys.*, *37*, 1219–1222, doi:10.1016/0021-9169(75)90193-2.

Bilitza, D. (1987), Description of the mean behavior of ionospheric plasma temperature, *Adv. Space Res.*, *7*(6), 93–98, doi:10.1016/0273-1177(87)90280-8.

Bilitza, D., and W. R. Hoegy (1990), Solar activity variation of ionospheric plasma temperatures, *Adv. Space Res.*, *10*(8), 81–90, doi:10.1016/0273-1177(90)90190-B.

Bilitza, D., V. Truhlik, P. Richards, T. Abe, and L. Triskova (2007), Solar cycle variation of mid-latitude electron density and temperature: Satellite measurements and model calculations, *Adv. Space Res.*, *39*, 779–789, doi:10.1016/j.asr.2006.11.022.

Brace, L. H., and R. F. Theis (1978), An empirical model of the interrelationship of electron temperature and density in the daytime thermosphere at solar minimum, *Geophys. Res. Lett.*, *5*, 275–278, doi:10.1029/GL005i004p00275.

Dalgarno, A., and M. B. McElroy (1965), Ionospheric electron temperatures near dawn, *Planet. Space Sci.*, *13*, 143–145, doi:10.1016/0032-0633(65)90183-2.

Evans, J. V. (1971), Millstone Hill Thomson scatter results for 1967, *Tech. Rep. 482*, Lincoln Lab., Mass. Inst. of Technol., Lexington, Mass.

Evans, J. V. (1973), Millstone Hill Thomson scatter results for 1966 and 1967, *Planet. Space Sci.*, *21*, 763–792, doi:10.1016/0032-0633(73)90095-0.

Fejer, B. G. (1991), Low latitude electrodynamic plasma drifts: A review, *J. Atmos. Terr. Phys.*, *53*, 677–693, doi:10.1016/0021-9169(91)90121-M.

Hedin, A. E., and H. G. Mayr (1987), Solar EUV induced variations in the thermosphere, *J. Geophys. Res.*, *92*, 869–875, doi:10.1029/JD092iD01p00869.

Hirao, K., and K.-I. Oyama (1970), An improved type of electron temperature probe, *J. Geomag. Geoelectr.*, *22*, 393–402, doi:10.5636/jgg.22.393.

Hoegy, W. R. (1984), Thermal electron heating rate: A derivation, *J. Geophys. Res.*, *89*, 977–985, doi:10.1029/JA089iA02p00977.

Kakinami, Y., S. Watanabe, and K.-I. Oyama (2008), An empirical model of electron density in low latitude at 600 km obtained by Hinotori satellite, *Adv. Space Res.*, *41*, 1495–1499, doi:10.1016/j.asr.2007.09.031.

Kakinami, Y., C. H. Chen, J. Y. Liu, K.-I. Oyama, W. H. Yang, and S. Abe (2009), Empirical models of total electron content based on functional fitting over Taiwan during geomagnetic quiet condition, *Ann. Geophys.*, *27*, 3321–3333, doi:10.5194/angeo-27-3321-2009.

Kakinami, Y., N. Balan, J. Y. Liu, and K.-I. Oyama (2010), Predawn ionospheric heating observed by Hinotori satellite, *J. Geophys. Res.*, *115*, A01304, doi:10.1029/2009JA014334.

Kakinami, Y., C. H. Lin, J. Y. Liu, M. Kamogawa, S. Watanabe, and M. Parrot (2011), Daytime longitudinal structures of electron density and temperature in the topside ionosphere observed by the Hinotori and DEMETER satellites, *J. Geophys. Res.*, *116*, A05316, doi:10.1029/2010JA015632.

Lei, J., L. Liu, W. Wan, and S.-R. Zhang (2005), Variations of electron density based on long-term incoherent scatter radar and ionosonde measurements over Millstone Hill, *Radio Sci.*, *40*, RS2008, doi:10.1029/2004RS003106.

Lei, J., R. G. Roble, W. Wang, B. A. Emery, and S.-R. Zhang (2007), Electron temperature climatology at Millstone Hill and Arecibo, *J. Geophys. Res.*, *112*, A02302, doi:10.1029/2006JA012041.

Mantas, G. P. (1975), Theory of photoelectron thermalization and transport in the ionosphere, *Planet. Space Sci.*, *23*, 337–354, doi:10.1016/0032-0633(75)90139-7.

Moffett, R. J., and W. B. Hanson (1965), Effect of ionization transport on the equatorial *F* region, *Nature*, *206*, 705–706, doi:10.1038/206705a0.

Nagy, A. F., and P. M. Banks (1970), Photoelectron fluxes in the ionosphere, *J. Geophys. Res.*, *75*, 6260–6270, doi:10.1029/JA075i031p06260.

Namba, S., and K.-I. Maeda (1939), *Radio Wave Propagation*, 86 pp., Corona, Tokyo.

Oya, H., T. Takahashi, and S. Watanabe (1986), Observation of low latitude ionosphere by the impedance probe on board the Hinotori satellite, *J. Geomag. Geoelectr.*, *38*, 111–123, doi:10.5636/jgg.38.111.

Oyama, K.-I., N. Balan, S. Watanabe, T. Takahashi, F. Isoda, G. J. Bailey, and H. Oya (1996a), Morning overshoot of T_e enhanced by downward plasma drift in the equatorial topside ionosphere, *J. Geomag. Geoelectr.*, *48*, 959–966, doi:10.5636/jgg.48.959.

Oyama, K.-I., S. Watanabe, Y. Su, T. Takahashi, and K. Hirao (1996b), Season, local time, and longitude variations of electron temperature at the height of ~600 km in the low latitude region, *Adv. Space Res.*, *18*(6), 269–278, doi:10.1016/0273-1177(95)00936-1.

Oyama, K.-I., T. Abe, K. Schlegel, A. Nagy, J. Kim, and K. Marubashi (1999), Electron temperature measurement in Martian ionosphere, *Earth Planets Space*, *51*, 1309–1317.

Ren, Z., W. Wan, L. Liu, B. Zhao, Y. Wei, X. Yue, and R. A. Heelis (2008), Longitudinal variations of electron temperature and total ion density in the sunset equatorial topside ionosphere, *Geophys. Res. Lett.*, *35*, L05108, doi:10.1029/2007GL032998.

Schunk, R. W., and A. F. Nagy (1978), Electron temperatures in the *F* region of the ionosphere: Theory and observations, *Rev. Geophys.*, *16*, 355–399, doi:10.1029/RG016i003p00355.

Watanabe, S., and K.-I. Oyama (1996), Effects of neutral wind on the electron temperature at a height of 600 km in the low latitude region, *Ann. Geophys.*, *14*, 290–296, doi:10.1007/s00585-996-0290-5.

Zhang, S.-R., and J. M. Holt (2004), Ionospheric plasma temperature during 1976–2001 over Millstone Hill, *Adv. Space Res.*, *33*, 963–969, doi:10.1016/j.asr.2003.07.012.

Zhang, S.-R., J. M. Holt, A. M. Zalucha, and C. Amory-Mazaudier (2004), Midlatitude ionospheric plasma temperature climatology and empirical model based on Saint Santin incoherent scatter radar data from 1966 to 1987, *J. Geophys. Res.*, *109*, A11311, doi:10.1029/2004JA010709.

N. Balan and J.-Y. Liu, Institute of Space Science, National Central University, No. 300, Jhongda Rd., Jhongli 32001, Taiwan.

Y. Kakinami, Institute of Seismology and Volcanology, Hokkaido University, Kita 10 Nishi 8, Kita-ku, Sapporo 060-0810, Japan. (kakinami@mail.sci.hokudai.ac.jp)

S. Watanabe, Department of Cosmoscience, Hokkaido University, Kita 10 Nishi 8, Kita-ku, Sapporo 060-0810, Japan.